Environmental Science and Pollution Research (2023) 30:5799–5814
https://doi.org/10.1007/s11356-022-22549-0

RESEARCH ARTICLE

Interaction mechanism between nitrogen conversion and the microbial community in the hydrodynamic heterogeneous interaction zone

Lei Duan[1,2] · Jinghui Fan[1,2] · Yike Wang[1,2] · Yakun Wu[1,2] · Chenchen Xie[1,2] · Fei Ye[1,2] · Jiajia Lv[1,2] · Ming Mao[1,2] · Yaqiao Sun[1,2]

Received: 12 January 2022 / Accepted: 11 August 2022 / Published online: 18 August 2022

Abstract

To study the inorganic nitrogen in the process of interaction of river and groundwater and the changes in the microbial community, a vertical simulation device was used to simulate groundwater recharge to river water (upwelling) and river water recharge to groundwater (downwelling). The inorganic nitrogen concentrations in the soil and water solution as well as the characteristics of the microbial community were assessed to determine the inorganic nitrogen transformation and microbial community response in the heterogeneous interaction zone under hydrodynamic action, and the interaction mechanism between nitrogen transformation and the microbial community in the interaction zone was revealed. The removal rates of NO_3^--N in the simulated solution reached 99.1% and 99.3% under the two fluid-groundwater conversion modes, and the prolonged hydraulic retention time (HRT) of the oxidization-reduction layer in the fine clay area and the high organic matter content made the inorganic nitrogen transformation process dominated by microorganisms more complete. The denitrification during upwelling, dominated by denitrifying bacteria in *Sphingomonas*, *Pseudomonas*, *Bacillus*, and *Arthrobacter*, was stronger than that during downwelling. Dissimilatory nitrate reduction to ammonium (DNRA), controlled by some aerobic bacteria in *Pseudomonas*, *Bacillus*, and *Desulfovibrio*, was more intense in downflow mode than upflow mode.

Keywords Hydrodynamic force · Heterogeneous interaction zone · Inorganic nitrogen transformation · Microbial community · River water-groundwater interaction

Introduction

Nitrogen plays an important role as one of the basic substances involved in the biogeochemical cycle (Tang et al. 2019). Due to the discharge of wastewater from intensive industrial and agricultural activities into rivers, nitrogen pollution, especially nitrate nitrogen pollution, has become increasingly serious (Li et al. 2017; Agarwal et al. 2019). Because of the physical, chemical, and biological differences between river water and groundwater, the groundwater-surface water (G-S) interaction zone can exhibit specific zoning patterns due to undercurrent belts, thus effectively removing some nitrogen, heavy metals, and organic matter through biogeochemical coupling (Su et al. 2019). Many scholars at home and abroad believe that the undercurrent interaction zone is a hot spot for inorganic nitrogen conversion (Vince et al. 2018; Valiente et al. 2018; Robert et al. 2014; Yu et al. 2021). Nitrate nitrogen pollution discharged into rivers will enter groundwater with the recharge process of river water. The complexity of nitrogen migration and transformation processes determines the complexity of groundwater nitrogen pollution (Zhao et al. 2021; Beggs et al. 2011). When the river level is lower than the groundwater level, the low-oxygen groundwater carries reducing substances to recharge the river (Marzadri et al. 2014). The heterogeneity of the medium in the interzone results in different flow paths, flow velocities, and retention times, which affect nitrogen conversion. Nitrogen transformation in the interzone was affected

Responsible Editor: Robert Duran

✉ Yaqiao Sun
48161587@qq.com

[1] School of Hydraulic Engineering and Environment, Chang'an University, Xi'an 710061, China

[2] Key Laboratory of Underground Hydrology and Ecological Effects in Arid Regions, Ministry of Education, Xi'an 710064, China

by soil particle properties (Wang et al. 2016). Using two-dimensional solute transport and sensitivity analysis, Shuai et al. (2017) concluded that the nitrogen reduction rate in lower seepage flow was controlled by factors such as the permeability coefficient of the medium layer and the fluctuation amplitude of the water level. Loosely structured interzones have a higher permeability coefficient, leading to an increase in nitrogen exchange capacity (Cao et al. 2021). The G-S interaction region generates physicochemical and biological gradients, resulting in differences in pH, dissolved oxygen (DO), organic matter content, and microbial community. Hou et al. (2012) simulated interaction zones at different depths by using columns and found that the nitrate nitrogen degradation rate was strongly correlated with organic matter, iron, and sulfur contents. In a study of nitrogen in the interaction zone, Duff and Triska (2000) found that redox action with DO as the main driving factor occurred in the nitrogen cycle. Through indoor sandbox experiments, Zhang et al. (2019) found that nitrification was positively correlated with the height of the groundwater level in the fluctuation zone, while denitrification was negatively correlated with this height. Zhang et al. (2014) pointed out that ammonia nitrogen in sediments tends to be released into anaerobic, weakly acidic water, while nitrate nitrogen tends to be released into aerobic alkaline water. Studies have shown that denitrifying bacteria and ammonia-oxidizing bacteria are related to the inorganic nitrogen level and hydrochemical factors in the interaction zone (Repert et al. 2015; Tatariw et al. 2013). Liu et al. (2015) believed that the abundance of ammonia-oxidizing archaea (AOA) and ammonia-oxidizing bacteria (AOB) of nitrifying bacteria increased during the groundwater level cycle and decreased when the Eh value was low; AOA were more adaptable than AOB to the low-oxygen environment in the fluctuating water level zone. Zhao and Liu (2018) pointed out that nitrate nitrogen tends to accumulate in the partial reduction area at the lower level of the fluctuation zone, resulting in an increase in the abundance of denitrifying bacteria at this level and a strong denitrification effect. Stonedahl et al. (2018) pointed out that changes in chemical components, DO, redox potential, organic matter content, and other physical and chemical properties in the media in the interaction zone would make the microbial community structure respond accordingly.

Most studies have focused on the migration and transformation of nitrate nitrogen in the G-S interaction zone and mainly analyzed nitrogen transformation and the microbial community distribution in the interaction zone. However, the mechanisms of nitrogen transformation and microbial community interactions in heterogeneous interaction zones under different hydrodynamic conditions are poorly understood. Therefore, on the basis of field investigation, this article uses an interaction zone simulation device to study the different infiltration processes of upflow and downflow, the migration and transformation trends of inorganic nitrogen in the interaction zone, and the change characteristics of the microbial community in the interaction zone and to predict the function of microorganisms. Furthermore, this study establishes a conceptual model of the transformation of inorganic nitrogen in the heterogeneous interaction zone under different hydrodynamic conditions and explores the mechanism of interaction between the transformation of inorganic nitrogen and the microbial community to provide a reasonable basis for the comprehensive treatment and remediation of nitrogen pollution in water bodies.

Material and methods

Sample collection and testing

The Wei River is the largest tributary of the Yellow River, which is also an important economic core area and ecological corridor of the Loess Plateau. In this paper, the Xi'an section of the Wei River Basin was selected as the research area to explore the migration and transformation of inorganic nitrogen in the G-S interaction zone. The sediments in the interaction zone in the sampling area are mainly composed of silt, coarse, sand and clay in alternating fashion. According to the particle size (PZ) analysis of the screened soil, the soil can be divided into three types: gravel ($PZ > 2$ mm), sand (0.075 mm $< PZ < 2$ mm), and clay or silt ($PZ < 0.075$ mm) (Song et al. 2009). According to the classification criteria of soil types, the in situ soil depth profile of sample #1 was 0–50-cm silt, 50–110-cm clay, and 110–200-cm coarse sand. Soil profile #1 was selected as the research object.

Samples were collected in November 2019, including river water, groundwater, and lateral interaction zone soil samples. Before sampling Weihe River water, the sampling bottle was repeatedly wetted and washed with river water, and the sample was taken from flowing water (Fig. 1) . Groundwater samples were taken from groundwater monitoring wells at a low speed to avoid the impact of fluctuations on water sample indexes during pumping. Before sampling, parameters such as the Eh, DO, pH, total organic carbon (TOC), and temperature of water samples were monitored until the parameters were stable, after which the groundwater samples were collected, and the stable parameters were recorded. Soil samples in the interaction zone were collected at a depth of 200 cm and loaded into sterile sampling bags for the determination of in situ soil microbial communities. The microbial indexes were analyzed by Sangon Biotech (Shanghai).

The original soil sample (#1) from the interaction zone was naturally dried indoors, and extraneous materials were removed. The soil for the experiment was prepared

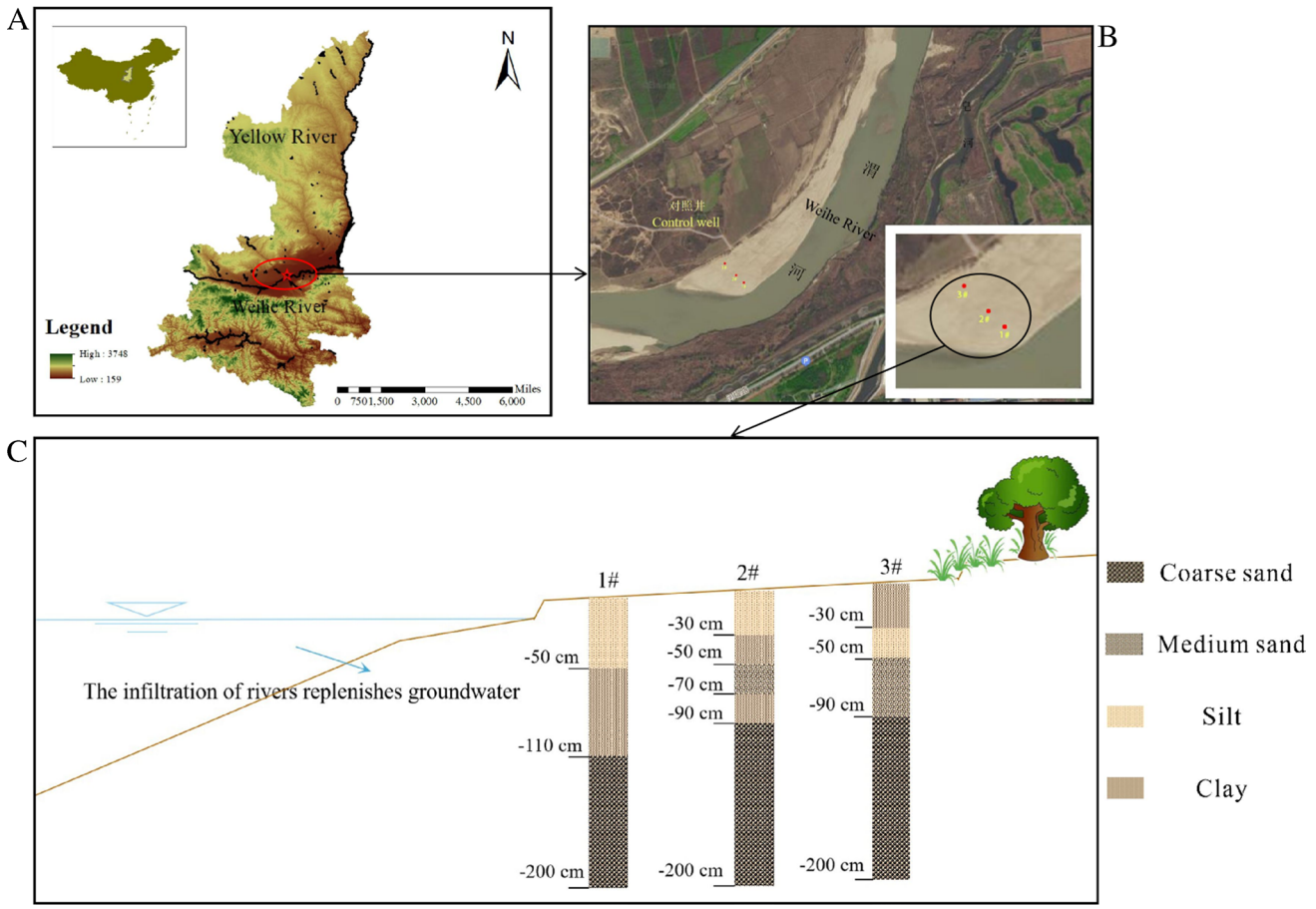

Fig. 1 **A**) Location of study area. **B**) Satellite map of the sampling point. **C**) Sampling point profile location

by screening through 200 mesh and 8 mesh and filled proportionally according to the actual stratification situation of site #1. After the groundwater and river water samples were filtered through a 0.45-μm membrane, the concentration of NH_4^+ was determined by colorimetry, the concentration of NO_2^- was determined by N-1-naphthyl-ethylenediamine dihydrochloric acid spectrophotometry, and the concentration of NO_3^- was determined by ultraviolet spectrophotometry. The dried soil was placed in water at a solid–liquid ratio of 1:2.5 and shaken for 24 h to determine the pH and oxidation–reduction potential (ORP) of the soil samples. The KCl extraction method was used to extract the soil samples, and then the supernatant was filtered to determine NO_2^-, NO_3^-, and NH_4^+ after centrifugation.

Experimental method

Experimental device

To study the migration and transformation of inorganic nitrogen in the interaction zone under different hydrodynamic conditions, a simulation device for the G-S interaction zone was designed as shown in Fig. 2. Two plexiglass columns and two pressure gauges were designed and implemented according to the actual situation of the in situ test site. The plexiglass column was 80 cm high and 20 cm in diameter, the upper and lower parts were sealed with lids, and the water inlet and outlet were on the left side. There were 7 sampling pipes on the left side of the column, each 10 cm apart. There were 13 pressure measuring tubes on the right side, and each tube opening was 5 cm apart. The pressure measuring plate was 120 cm high and 80 cm wide. The pressure plate scale corresponded to the pressure of the tube used for the simulated soil column.

Quartz sand with a thickness of 5 cm was added at the top and bottom of the soil column to prevent water from impacting the soil layer and blocking the water outlet. After air drying, the soil sample was loaded into the soil column. After media filling, the column was first filled with distilled water, and the water entered slowly from the lower end. According to the soil particle size and the size of the soil column simulation device, the height of water head is controlled between ± 40 and ± 80 cm to avoid the pore and fissure caused by water head impacting the soil column. When

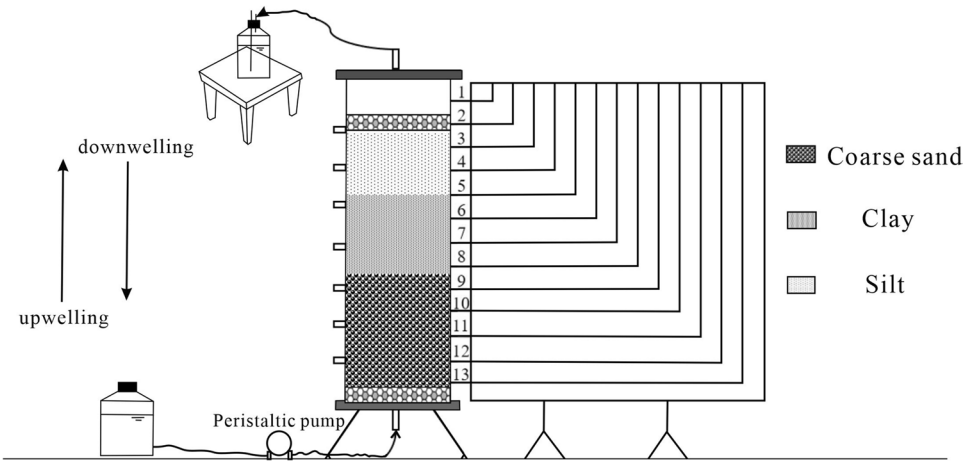

Fig. 2 Experimental setup

the soil column was completely immersed with water, water saturation was reached, and gravity drainage occurred. The saturation and gravity drainage steps were repeated until the sand thickness is stabilized. Finally, distilled water was added to reach the design height.

To avoid the influence of temperature and illumination on the experimental results, a dark environment was maintained during the experiment, and the temperature was controlled at 25–30 °C. When taking water samples, the sampling bottle was filled with argon gas to prevent NO_2^- from being oxidized by O_2 in the air during the sampling process. The experiment was divided into early stage and late stage. In the early stage, the concentration fluctuated greatly. Water samples were measured every day for 18 days. In the later period, the concentration fluctuation range was small, and water samples were measured every 2 days for 14 days. The test indexes of the water samples included pH, DO, ORP, and the concentrations of NH_4^+, NO_2^-, and NO_3^-, and the change in water level was recorded. At the end of the experiment, soil samples at different depths were taken from the lateral sampling ports of the plexiglass column, and the measurement indexes included microorganisms, pH, TOC, and NH_4^+, NO_2^-, and NO_3^- concentrations.

To ensure the accuracy of the experimental data, a blank sample was set for the determination of inorganic nitrogen in the effluent water samples, and the water sample and soil data were tested three times. Samples for microbial analysis were bagged, stored in a BDF-86H50 medical cryopreservation box for freeze-drying, and later sent to Sangon Biotech (Shanghai) for microbial classification and sequencing.

Analog fluid configuration

According to the measured index values of river and groundwater samples, simulated river and groundwater samples were used for the upwelling and downwelling soil column simulation experiments. The components of the two experimental simulated fluids are shown in Table 1. The groundwater flow rate is slow, the runoff path is long, and DO is consumed by biogeochemical reactions in the runoff process, so the DO content in groundwater is usually low. DO content is an important factor affecting nitrogen migration and transformation, so DO was selected as the difference index to distinguish simulated river water from simulated groundwater. The DO content in the simulated groundwater was less than 2 mg/L.

Table 1 Simulated water sample configuration

Experiment	Simulated fluid	CH_3COONa (mg/L, in terms of C)	$NaNO_3$ (mg/L, in terms of N)	NH_4Cl (mg/L, in terms of N)
Upwelling	Groundwater	98	91	——
Downwelling	Surface water	98	66	6

Calculation of hydrodynamic parameters of the heterogeneous interaction zone

The hydrodynamic parameters to be calculated in this study are permeability coefficient, seepage velocity, and hydraulic residence time (HRT).

The vertical permeability coefficient of the interaction zone was calculated according to the simplified calculation formula for the vertical permeability coefficient proposed by Chen (2007):

$$K_Z = \frac{L}{t_2 - t_1} \ln\left(\frac{h_1}{h_2}\right) \quad (1)$$

If the seepage velocity is expressed as the seepage flow per unit time, then the seepage velocity is proportional to the first power of the hydraulic gradient:

$$V = K_Z J \tag{2}$$

The formula for calculating hydraulic retention time (HRT) is as follows:

$$HRT = \frac{L}{V} \tag{3}$$

where K_z is the vertical permeability coefficient (m/d), L is the thickness of different media in the plexiglass column (cm), t is time (d), and h is the height of the water level at a given time (m).

Data analysis

Origin 2021 software was used to process and analyze the data. In the process of microbial diversity analysis, the Ace and Chao indices were used to reveal the richness of the soil microbial community, and the Shannon index was used to reveal the diversity of the soil microbial community. FAPROTAX database data were used to predict microbial community functions, and the predicted values were combined with grayscale mapping to obtain the functional characteristics of soil microorganisms at different depths in the upwelling and downwelling experiments. To further obtain the functional characteristics of soil microorganisms at different depths in upwelling and downwelling experiments, the FAPROTAX database was used to predict microbial community functions. Each operational taxonomic unit (OTU) sequence involved in function prediction corresponded to either one function or multiple functions. Each listed nitrogen conversion function was detected at a certain level. To make the results more intuitive, values ≥ 352 are marked; there are other values that are not shown, but the value is relatively low, and a trend is not obvious.

Results and discussion

Hydrodynamic characteristics of the heterogeneous interaction zone

Calculation of permeability coefficient

According to the vertical permeability coefficient calculation of different soil types in Table 2, it can be seen that the permeability coefficient of soil with different particle sizes varies greatly, which has a certain impact on water flow velocity and HRT in the interactive zone.

Distribution characteristics of seepage velocity and hydraulic residence time

The flow velocity and HRT of silt, clay, and coarse sand were calculated according to the variation in the water level in the simulated interaction zone. In silt soils, especially cohesive soils, due to the large specific surface area and small pores of the soil, it is difficult for water flow to pass through clay porous media under low hydraulic gradients. Taking the simulated downflow process as an example, the average seepage velocity was 0.01 m/d in the clay soil area of the plexiglass column, which was significantly lower than the average seepage velocities of 0.40 m/d in the coarse sand area and 0.10 m/d in the silt area. The average HRT was 8.40 d, which was approximately 8 times that of the silt area and 30 times that of the coarse sand area. The flow velocity of percolation in the coarse sand zone at the bottom of the plexiglass column was the lowest, with a value of only 0.28 m/d. It has been pointed out that the heterogeneity of lateral interaction zones leads to differences in vertical permeability coefficients, which affect water flow exchange and solute residence time, thus affecting the degree of nitrogen removal (Tonina et al. 2016). However, the removal of NO_3^- in the heterogeneous interaction zone under flow conditions is usually difficult to characterize by field observations because the nitrogen concentration and reaction dynamics can change over a short distance and a short period of time. Sawyer and Cardenas (2009) conducted numerical simulation analysis on equivalent homogeneous and heterogeneous sediment layers, and the results showed that heterogeneity would change the solute transport rate and affect solute transport behavior. Water has a short residence time in sandy soils and a long residence time in organic-rich clays, consuming oxygen and forming reduction zone conditions that promote nitrate removal (Barnes et al. 2019; Yabusaki et al. 2017). The percolation flow velocity at the bottom of the plexiglass column was low, only 0.28 m/d, which may be caused by the increase in pressure between the media, which causes particle redistribution in the permeating medium, and the narrowing of the percolation channel, which affects the percolation form of the medium and deviates from the maximum value (Wang et al. 2019). Other studies have shown that with increasing seepage velocity, the decrease in permeability rate in the medium is caused by the increase in eddy current between particles in the soil medium (Fig. 3) . The laminar flow boundary becomes narrower, and the permeability coefficient decreases, thus deviating from Darcy's law (Chaudhary et al. 2011).

Table 2 Vertical permeability coefficients of different soil types

Agrotype	Silt	Clay	Coarse sand
Vertical permeability coefficient (m/d)	1.3×10^{-3}	9.9×10^{-4}	2.3×10^{-2}

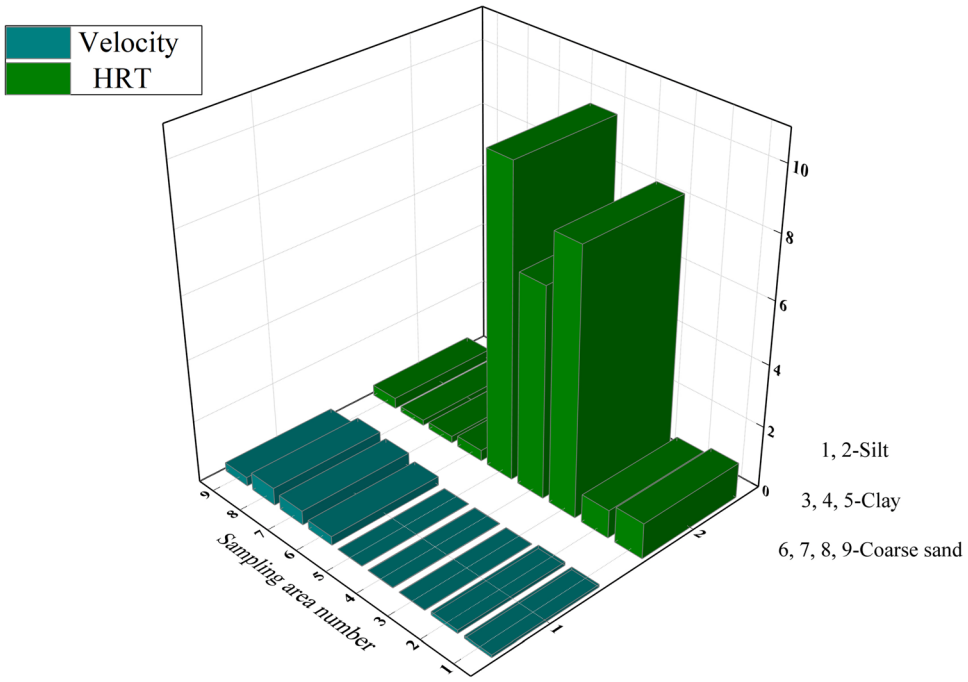

Fig. 3 Flow rate and HRT profile. Parameters: 1—#3 ~ #4; 2—#4 ~ #5; 3—#5 ~ #6; 4—#6 ~ #7; 5—#7 ~ #8; 6—#9 ~ #10; 7—#10 ~ #11; 8—#11 ~ #12; 9—#12 ~ #13

Concentration variation characteristics of inorganic nitrogen in the interaction zone under various hydrodynamic conditions

Variation characteristics of inorganic nitrogen concentrations in the experimental effluent

The upwelling and downwelling flow simulation experiment lasted for 32 days. As shown in the diagram of NO_3^--N over time (Fig. 4A), the trend of NO_3^- concentration in upflow and downflow conditions was relatively consistent, rising first and then declining. In the later stage of the experiment, the NO_3^- concentration gradually became stable. Before the experiment, the sediment column was saturated with deionized water. When the simulated water sample entered the saturated soil column, the pore water in the soil medium dispersed and mixed, leading to an increase in NO_3^- concentration to a peak. At the late stage of the experiment, the NO_3^- concentration in the upflow and downflow experiments was significantly reduced compared with that in the simulated liquid, and the NO_3^- removal rate reached 99.1% and 99.3%, respectively. Duan (2010) cultured soils of different

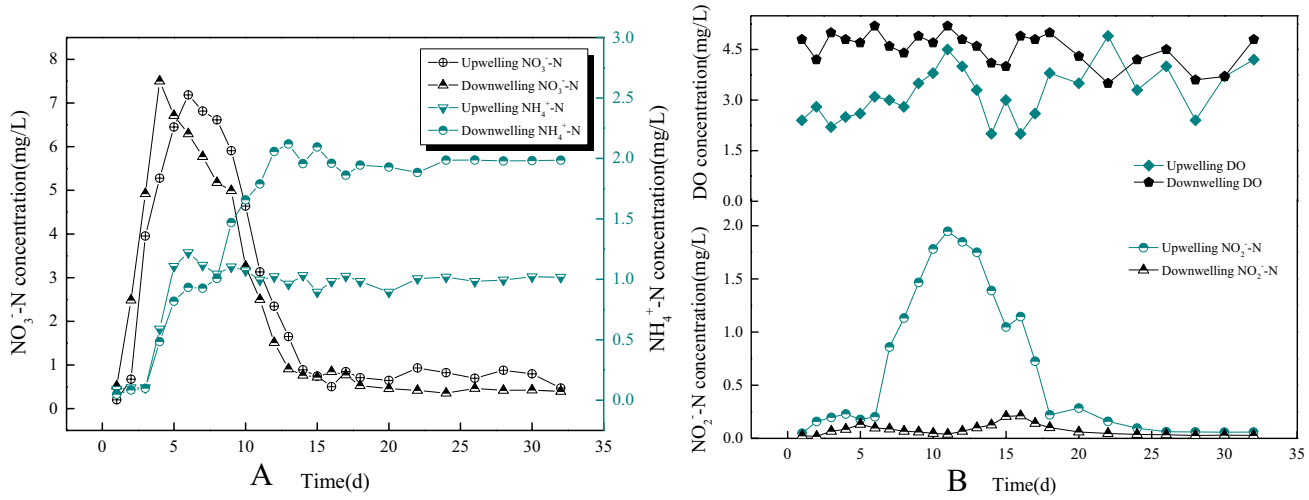

Fig. 4 **A**) Changes in NO_3^- and NH_4^+ concentrations in water from upwelling and downwelling tests. **B**) Changes in NO_2^- concentration in water from upwelling and downwelling flow experiments

soil types in serum bottles to study the natural attenuation of nitrate nitrogen in simulated aquifers with loess, silt, silty clay, and silt as media. The average reduction rates of nitrate nitrogen in the experimental period were 38.18%, 37.52%, 37.02%, and 28.32%, respectively. This result indicates that the NO_3^- carried by upwelling and downwelling flows in this experiment has a good removal effect in the simulated interaction zone. The variation trend of NO_2^- concentration in the upwelling experiment showed an obvious peak with a trend of rising first and then falling (Fig. 4B). Denitrification gradually reduces NO_3^- to NO_2^-, N_2O, and N_2. The first step of the denitrification process is that the *narG* gene encodes membrane-bound nitrate reductase, which can catalyze the reduction of nitrate to nitrite; the *nirS* and *nirK* genes encode nitrite reductase, which reduces nitrite to NO, which is a rate-limiting step in the denitrification process (Ma et al. 2014; Ge et al. 2012). The synthesis of nitrate reductase occurs earlier than that of nitrite reductase, the reduction of NO_3^- occurs preferentially, and the temporary accumulation of NO_2^- occurs. The concentration of NO_2^- in downwelling flow was always lower than 0.25 mg/L, and after 15 days, the concentration of NO_2^- in upwelling flow began to decrease and approached 0 mg/L. The decrease in NO_2^- concentration may be caused by anammox or continued denitrification, which converts NO_2^- into N_2. The DO content in overlying water is closely related to the denitrification intensity. Shao et al. (2008) noted that when DO is greater than 4.2 mg/L, the denitrification rate decreases; when the DO level reached 5.6 mg/L, denitrification contributed only 4% to NO_3^- attenuation. The DO value of upflow was higher than that of downflow, and the NO_2^- accumulation-consumption effect was obvious, indicating that the denitrification in upflow conditions was more intense. Under the action of upwelling and downwelling, NH_4^+ gradually accumulated and tended to be stable. Effluent NH_4^+ in the upwelling scenario showed an upward trend during the third to sixth day and stabilized at 1 ± 0.1 mg/L after the sixth day. The effluent concentration of NH_4^+ in the downwelling scenario showed an upward trend in the first 12 days and rose to 2.16 mg/L on the twelfth day. The concentration of NH_4^+ in the experimental effluent remained stable at 2.0 ± 0.12 mg/L in the later period (Fig. 4A). NO_3^- is converted to NH_4^+ through dissimilatory nitrate reduction to ammonium (DNRA). The specific process is that bacteria convert NO_3^- to NO_2^- through the nitrate dissimilation reductase *Nar* and then reduce NO_2^- to NH_4^+ through *Nir*. DNRA changes the morphology of nitrite, but removal cannot be achieved (Kraft et al. 2011). Organic nitrogen mineralization transforms organic nitrogen in the soil medium into NH_4^+ and increases the concentration of NH_4^+. Yan et al. (2017) found in a simulation experiment that among the considered effects, the contribution of DNRA to upwelling effluent NH_4^+ was as high as 71%, while the contribution to the downwelling effluent value was only 11%. The DO carried by the upflow simulation solution was only 1 mg/L after high-purity Ar aeration, and the DO concentration of the experimental effluent fluctuated at approximately 2 mg/L. The DO concentration in the water was lower than that in the downflow experiment, which was conducive to the occurrence of organic nitrogen mineralization, but the effect of DRNA was weak. A low-DO state is conducive to the release of NH_4^+ from sediment organic nitrogen mineralization to the water body (Li et al. 2012). The concentration of NH_4^+ in the experimental effluent was affected by the intensity of DRNA and organic nitrogen mineralization.

Characteristics of inorganic nitrogen concentration in soils in heterogeneous interaction zones

After 32 days of hydrodynamic activity, the total nitrogen content in the simulated heterogeneous interaction zone in the soil column increased significantly. As shown in Fig. 5, the content in upwelling soil increased by 2–11 times, and that in downwelling soil increased by 4–11 times, indicating that more nitrogen was absorbed by the soil medium under downwelling than upwelling. The increases in NO_3^--N and NO_2^--N were small, and the nitrogen absorbed by the medium was mainly NH_4^+-N. In downflow mode, the soil retention of NH_4^+-N produced by the action of DRNA was stronger than that in upflow mode. The reason may be that DRNA has a significant effect in downflow conditions, and particles that easily adsorb cations in the medium accumulate and adsorb cations, while in upflow, mineralization may dominate the organic nitrogen reactions, and the NH_4^+-N released by organic nitrogen mineralization is less than that released by DRNA. Except for the − 30-cm and − 40-cm clay particle layers, the interception of NH_4^+ decreased gradually with the direction of water flow, and the interception effect was relatively good at the water-soil interface layer. This observation is consistent with Wu Chao's (2019) study, which showed that the NH_4^+-N content in experimental soil under negative-pressure irrigation decreased with increasing infiltration distance. The increase in NH_4^+ at the − 30-cm and − 40-cm clay particle layers was greater than that in the silt and coarse sand layers, and the increase in NH_4^+-N at − 30 cm and − 40 cm under downflow reached 228 mg/kg and 288 mg/kg, respectively. The increase in NH_4^+-N at − 30 cm and − 40 cm under upwelling reached 172 mg/kg and 196 mg/kg, respectively, which was much higher than that in other regions. The nonlinear adsorption of NH_4^+ depends on the concentration of NH_4^+ in pore water (Rassam et al. 2006). More adsorption sites for NH_4^+-N generated by DRNA and organic nitrogen mineralization are available in fine particle areas with a high organic matter content. In clay layers, the water level difference is small, the water head gradient leads to a slow flow rate, and the

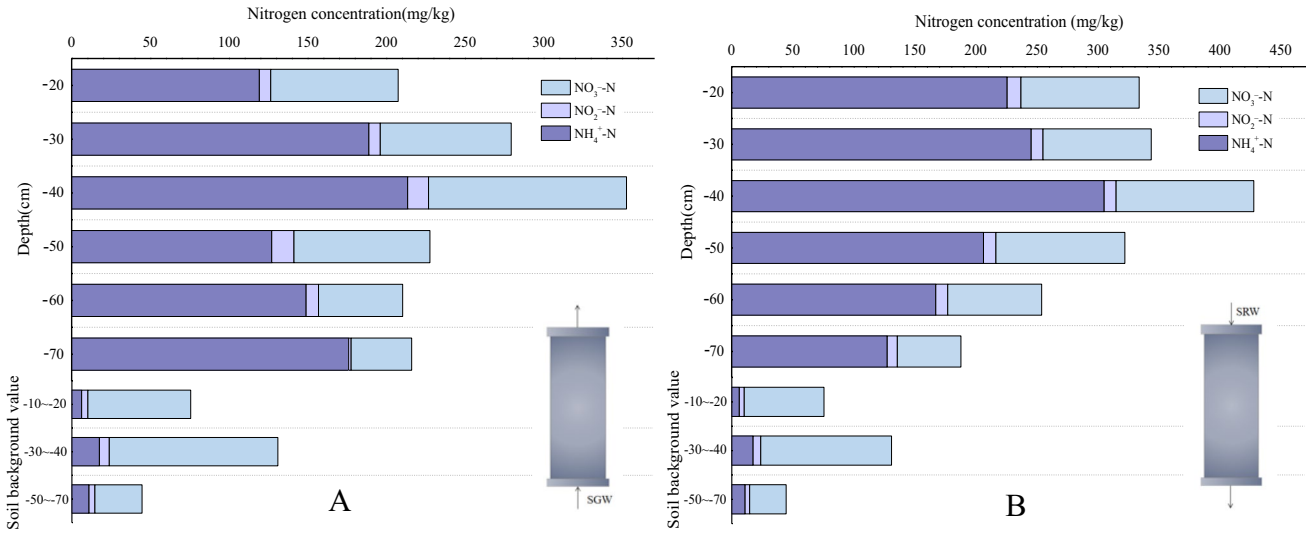

Fig. 5 **A**) Characteristics of soil nitrogen content in downflow conditions. **B**) Characteristics of soil nitrogen content in upflow conditions

Table 3 Simulated soil column nitrogen migration and transformation zones

Upwelling		Downwelling		Reaction type
Depth	Redox zone	Depth	Redox zone	
0 ~ − 20 cm	Weak oxidation zone	0 ~ − 20 cm	Oxidation zone	Nitrification
− 20 ~ − 50 cm	Oxidation–reduction zone	− 20 ~ − 40 cm	Oxidation–reduction zone	Nitrification, denitrification, DRNA
− 50 ~ − 70 cm	Reduction zone	− 40 ~ − 70 cm	Weak reduction zone	Denitrification, DRNA

prolonged HRT promotes DNRA or organic nitrogen mineralization, providing sufficient conditions to remove nitrate through biogeochemistry. HRT is an important factor affecting the nitrate decay rate, which is consistent with the study of Yuanyuan et al. (Liu et al. 2017).

Redox zone characteristics and microbial response across zones

Division of redox zones

After the simulated river water passed through the interaction zone, the maximum DO concentration increased to 6.2 mg/L, while the DO concentration of the simulated groundwater was always lower than 3.5 mg/L after soil action, which corresponds to a low state of DO. The groundwater simulation fluid under upwelling was in an anoxic interaction zone, while that under downwelling was in an aerobic environment. The effluent pH of both the upwelling and downwelling tests was higher than 7, showing weak alkalinity. The effluent pH of the downwelling tests was slightly higher than that of the upwelling tests. The average redox potential for upflow was lower than that for downflow. The reduction environment in the upflow interaction zone was more intense, and the ability to accept electrons was stronger. TOC provides energy for microbial activity. The variation trend in soil TOC is shown in the following figure, with silt at − 20 cm, fine clay particles at − 30 ~ − 40 cm and coarse sand at − 50 ~ − 70 cm. In general, more organic mass was consumed under upwelling than under downwelling, and microbial activity was intense during upwelling.

The nitrogen migration and oxidation zones corresponded to the inorganic nitrogen content, DO, and redox potential of soil samples at different depths in the heterogeneous soil column simulation device, as shown in Table 3.

Table 3 shows that within the range of 0 ~ − 70 cm in the simulated soil column, the groundwater replenishment of river water can be divided into a weak oxidation zone, oxidation–reduction zone, and reduction zone. In the reduction zone and weak reduction zone, different redox zones undergo different biochemical reaction processes. In the simulated upwelling experiment, the DO content of the water samples was relatively low, so the depth range of the reduction zone (− 40 ~ − 70 cm) was larger than that of the downflow reduction zone (− 50 ~ − 70 cm), and the depth range of the oxidation–reduction zone (− 20 ~ − 40 cm) was shorter than that

of the downflow oxidation–reduction zone (−20 ~ −50 cm). In the downflow experiment, due to the combined effects of the oxygen richness of the simulated river water and the oxidation of the interaction zone, the nitrification reaction dominated at 0 ~ −20 cm; this reaction consumes DO in the water, thereby reducing the DO value. The ORP value also decreased with depth, and, thus, the oxidation–reduction transition zone is located at −20 ~ −50 cm, where nitrification, denitrification, and DRNA mainly occur. The DO value gradually decreased in this region, and the NO_3^- and NO_2^- concentrations also tended to decrease because N_2O or N_2 is generated by denitrifying reduction reactions. The decrease in NO_3^- was also partly due to the contribution of DRNA. In the reduction zone (−50 ~ −70 cm), denitrification and DRNA mainly occur. When studying microbes in the shallow layer, Mermillod-Blondin et al. (2005) found that nitrification mainly occurred in the shallow layer of the interaction zone, and the shallow layer consumed the most oxygen. According to the TOC content in the interaction zone (Fig. 6), the TOC reduction of the upwelling soil sample at −20 ~ −50 cm was approximately 3 times higher than that of the upwelling soil sample at −50 ~ −70 cm, indicating that microbial activities in the upwelling −20 ~ −50 cm oxidation–reduction zone consumed more TOC. The TOC content in downflow exhibited little change in the weak reduction zone in the coarse sand area of −50 ~ −70 cm, and microbial activity was weak. In contrast, the total TOC consumption in upwelling was greater than that in downwelling, and there was a stronger microbial effect in upwelling.

Microbial responses to nitrogen transformation under hydrodynamic conditions

Studies have shown that different hydrodynamic effects can change the transport mode of nutrients and then affect the substrate concentration distribution and microshear environment, resulting in changes in microbial community structure (Zhong et al. 2017; Peng et al. 2014). Zhang (2019) pointed out that different hydrodynamic conditions can promote microbial participation in mediating a series of reactions related to nitrogen conversion. Soil samples at −20 cm, −40 cm, and −60 cm from the upwelling (S1, S2, S3) and downwelling (X1, X2, X3) tests were collected for microbial detection and analysis. The abundance and diversity of microorganisms in the experimental samples were higher than those in the in situ soil samples, indicating that hydrodynamic conditions can improve the abundance of microbial communities and promote the development of dominant bacteria. Upwelling samples S2 and S3 and downwelling samples X1 and X2 exhibited high abundance. Higher diversity was observed for samples S3 and X1 at the water-soil interface, which is subject to different hydrodynamic effects depending on the direction of water flow (Table 4).

At the phylum level, the dominant microflora were mainly *Proteobacteria*, *Firmicutes*, *Bacteroidetes*, and

Table 4 Microbial α diversity in sediment samples of hydrodynamic experiment

Sample	Chao	Ace	Shannon	Simpson
S1	1125.54	1342.39	0.50	0.057
S2	1803.34	1696.17	0.72	0.074
S3	1711.33	1706.26	0.80	0.09
Average	1546.74	1581.61	0.67	0.034
X1	1857.46	1843.71	0.82	0.05
X2	1746.31	1698.59	0.78	0.01
X3	1496.92	1493.03	0.67	0.05
Average	1700.23	1678.44	0.76	0.037

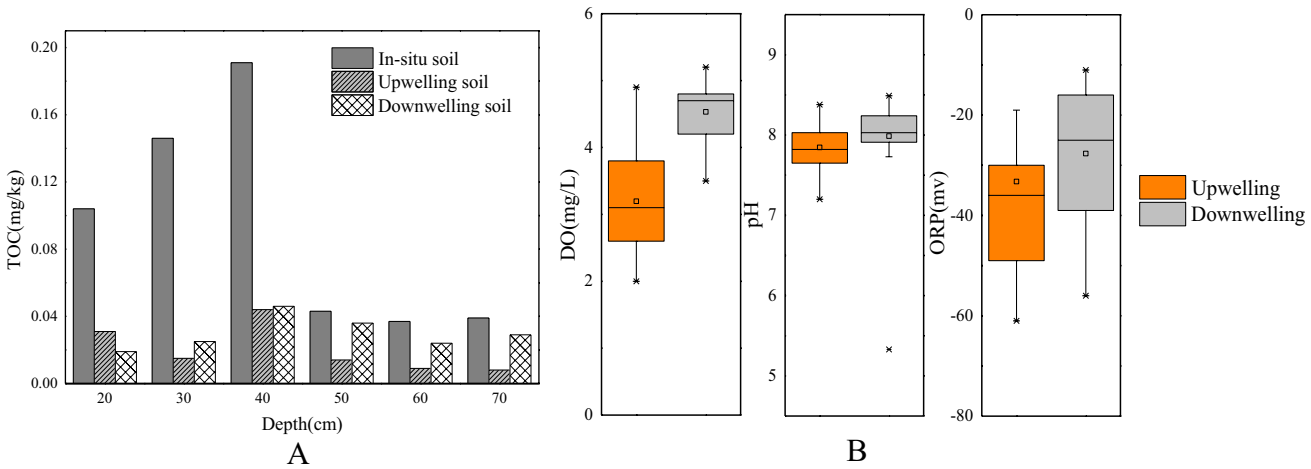

Fig. 6 **A**) TOC values of experimental soil samples. **B**) Basic physical and chemical properties of the effluent

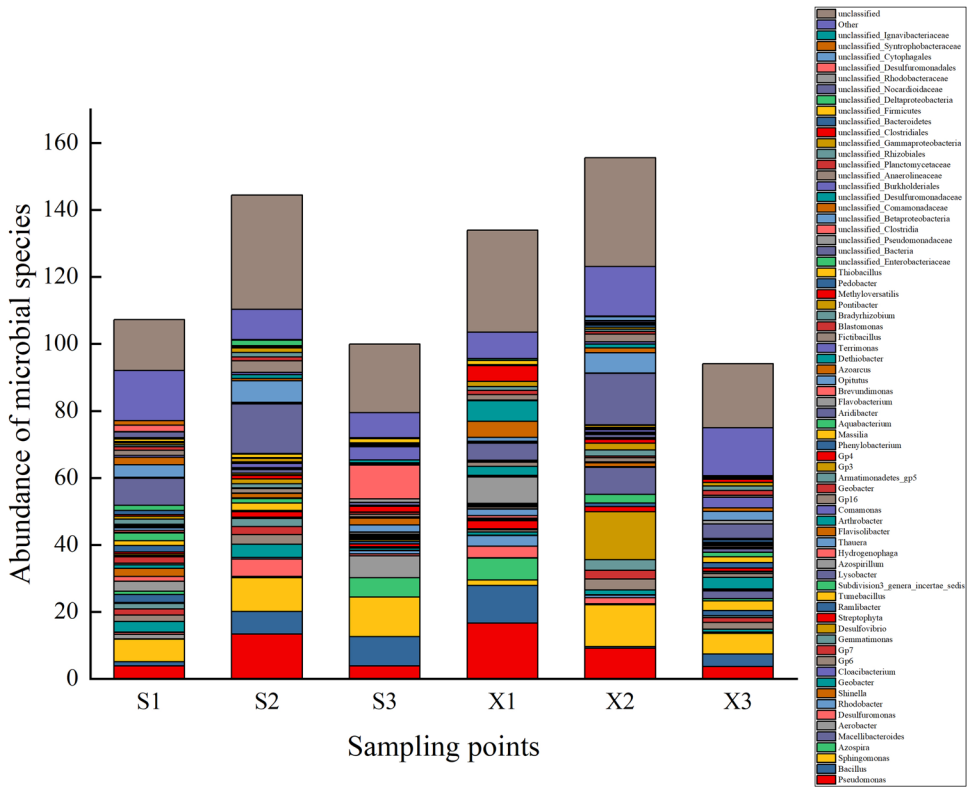

Fig. 7 Distribution characteristics of microorganisms under different hydrodynamic conditions

Table 5 Distribution characteristics of the microbial community in the interzone

Infiltration path	Depth	Soil type	Dominant bacterial groups	Abundance (%)
Upwelling	− 20 cm	Silt	*Sphingomonas*, *Pseudomonas*, *Geobacter*	12.7
	− 40 cm	Clay	*Pseudomonas*, *Sphingomonas*, *Bacillus*, *Desulfuromonas*	24.8
	− 60 cm	Coarse sand	*Sphingomonas*, *Bacillus*, *Aerobacter*, *Azospira*	27.3
Downwelling	− 20 cm	Silt	*Pseudomonas*, *Bacillus*, *Flavobacterium*, *Azospira*	31.8
	− 40 cm	Clay	*Desulfovibrio*, *Sphingomonas*, *Pseudomonas*, *Lysobacter*	28.7
	− 60 cm	Coarse sand	*Sphingomonas*, *Bacillus*, *Pseudomonas*	14.3

Planctomycetes, and the abundance of *Proteobacteria* accounted for approximately 1/2 of the abundance of dominant phyla. In the detection of microbial communities in other parts of China, *Proteobacteria* also showed clear superiority in sediments (Huang et al. 2019; Fang et al. 2014; Zhang et al. 2011). *Proteobacteria* and *Bacteroidetes* contain most of the 50 denitrifying bacteria genera that have been discovered (Chen et al. 2018). At the genus level, the dominant genera mainly included *Pseudomonas*, *Sphingomonas*, *Bacillus*, and *Azospira*. The hydrodynamic conditions at different depths of the interaction zone led to different environmental conditions in the media, resulting in a spatial distribution of dominant bacteria.

This study mainly selected the spatial distribution characteristics of microbial flora at the genus level for detailed analysis. As shown in Fig. 7 and Table 5, *Pseudomonas* and *Sphingomonas* were dominant at − 20 cm and 40 cm in upflow and performed denitrification. Some bacteria belonging to *Sphingomonas*, *Bacillus*, and *Aerobacter* that existed at the water-soil interface at − 60 cm have denitrification ability, and their abundance was as high as 27.3%. The interface area had sufficient carbon sources and enabled strong microbial reproductive ability. The abundance of the − 40-cm clay area under upwelling was 24.8%, and the fine particles with a high organic matter content promoted the growth and development of microorganisms. With upflow, *Pseudomonas*, a common denitrifying bacterium, was the dominant bacterium in the anoxic region of clay and coarse sand at depths greater than − 40 cm. According to Su et al. (2001), the relative abundance of *Pseudomonas* is strongly correlated with DO content, but denitrifying ability is not strongly correlated with DO. The anaerobic

Fig. 8 Microbial function prediction (FAPROTAX database)

environment in the interaction zone is more suitable for the survival of *Pseudomonas*. Under low DO, organic nitrogen mineralization by some bacteria of *Pseudomonas* and *Bacillus* can also occur (Li et al. 2012). *Desulfuromonas*, which was detected at − 20 cm under upflow, are mainly used for sulfate reduction in an anaerobic environment, while microbial metabolism provides energy for life activities. *Geobacter* was detected at − 20 cm under upwelling. Xu et al. (2008) pointed out that *Thiogenes*, iron-reducing bacteria in *Geobacter*, widely exist in anaerobic soils.

The DO of the downflow simulation fluid was higher than that of the upflow simulation fluid. With the progress of the simulation, the DO value gradually decreased, making DRNA flora more competitive. Studies have pointed out that when DO is reduced to severe hypoxia levels, the denitrification rate is reduced by 43%, the anammox rate is reduced by 38%, and the DRNA rate is three times as high as before (Song 2013). Pseudomonas was detected at all depths under downflow, and Bacillus was detected at − 20 cm and − 40 cm under downflow. Although Pseudomonas and Bacillus are common denitrifying bacteria, some of them have DRNA effects (Tao and Wen 2016). Therefore, the effect of DRNA in downflow was closely related to the oxygen content and the abundance of DRNA flora in soil samples at different depths. Desulfovibrio was the dominant species at − 40 cm under downflow and is mainly involved in some DRNA functions. Flavobacterium was detected at − 20 cm under downflow and is used for the degradation of some polycyclic aromatic hydrocarbons (PAHs) and for denitrification (Wu et al. 2008).

Bacillus and *Sphingomonas* have a strong ability to adapt to the environment and were detected in the coarse sand layer at − 60 cm under upwelling and downwelling, proving that they can survive in large quantities in coarse sand environments with a low organic matter content. *Azospira* was detected as the dominant bacterium under upflow at − 60 cm and under downflow at − 20 cm, and this bacterium belongs to *Betaproteobacteria* of the *Proteobacteria* and fixes N_2 in the air. The silt area at − 60 cm under upwelling and the coarse sand environment at − 20 cm under downwelling had a larger grain size than clay, and more abundant water flow at the soil–water boundary carried nutrients, which was more suitable for the growth and development of *Azospira*. This phenomenon is similar to the results obtained by Song et al. (2020) through correlation analysis: the abundance of nitrogen-fixing bacteria is significantly correlated with water and salt content. It can be seen that the characteristics of microbial communities in the heterogeneous interaction zone under upwelling and downwelling conditions are very different.

Figure 8 shows the function prediction results. The microbial denitrification functions related to nitrogen transformation mainly include nitrite and nitrate respiration, iron respiration, nitrate ammonification, nitrate reduction, and

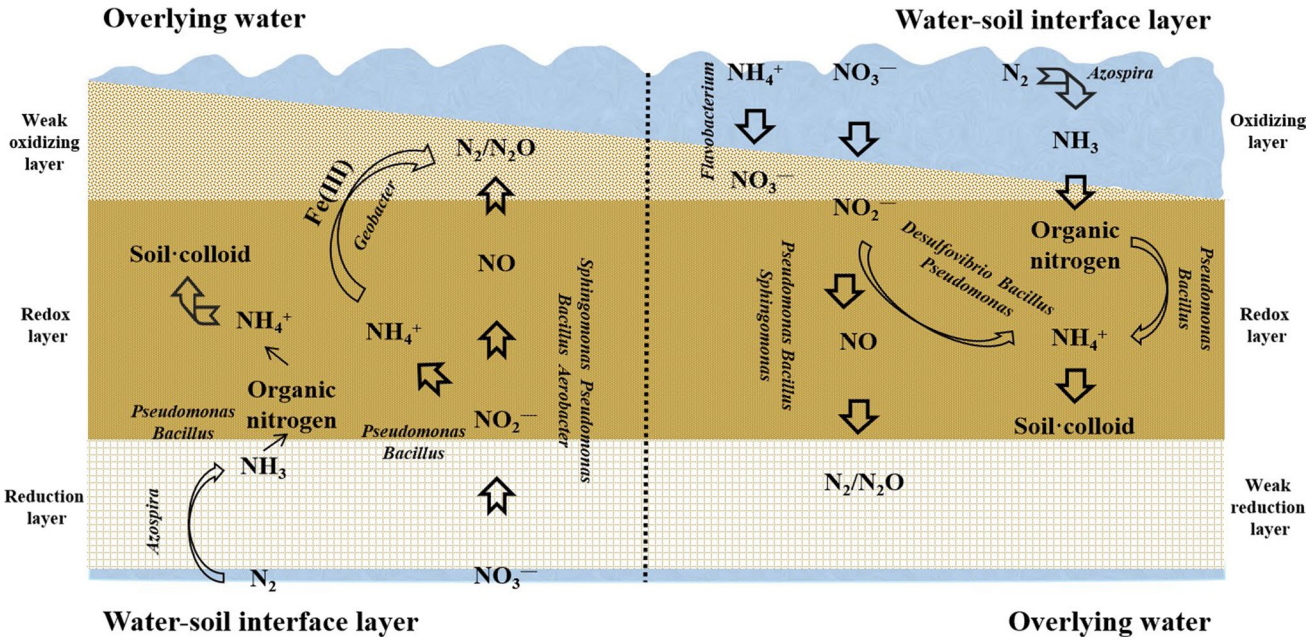

Fig. 9 **A**) Upwelling nitrogen conversion model. **B**) Downwelling nitrogen conversion model

nitrogen respiration. In addition, nitrification, nitrogen fixation, ammonification, and sulfate respiration occur. Sulfate respiration, a common reaction in nature, can provide energy for nitrogen-converting microbial activities. Overall, denitrification and DRNA were the main functions related to nitrogen conversion in upflow and downflow. The function distribution of each layer is shown in Fig. 8. Biological nitrogen fixation controlled by *Azospira* mainly occurred under upwelling at − 60 cm and under downwelling at − 20 cm at the water-soil interface. Nitrification controlled by *Flavobacterium* mainly occurred in the oxidation layer of − 20 cm in downflow. Ammoniation, that is, organic nitrogen mineralization, was more functional at − 20 cm and − 40 cm under upflow and was dominated by bacteria from *Pseudomonas* and *Bacillus*. Iron respiration occurred at − 20 cm under upwelling, which was mainly performed by *Thiogenes* (belong to *Geobacter*). There is a strong correlation between iron and nitrogen cycles, and coupling between Fe(III) and anammox exists (Zhuang et al. 2019). The presence of anammox in the function mapping results was strong, but anammox bacteria were not the dominant genera. The functional distribution of anammox was similar to that of iron respiration, which mainly occurred under strict anaerobic conditions under upwelling. Therefore, it is very likely that microorganisms used extracellular ammonia nitrogen as the terminal electron acceptor at − 20 cm under upwelling and reduced Fe(III) at the same time by oxidizing electron donors. This reaction mainly produces N_2, which can reduce the production of the greenhouse gas N_2O (Zhong et al. 2018) and store energy required for life activities. Nitrate ammonification, that is, DRNA, which is controlled by some aerobic bacteria in *Pseudomonas*, *Bacillus*, and *Desulfovibrio*, mainly took place in downflow. Nitrate denitrification, nitrate reduction, and nitrogen respiration were more intense at − 40 cm and − 60 cm under upwelling and downwelling; these processes are all related to denitrification. Denitrifying bacteria in *Pseudomonas*, *Bacillus*, *Sphingomonas*, and *Arthrobacter* were mainly responsible for denitrification, but denitrification was not strong at − 20 cm under downflow, and the relatively oxygen-rich conditions might limit the function of denitrifying bacteria. Denitrification under upflow gradually weakened with the direction of flow, and anammox and iron respiration gradually strengthened. Denitrification under downflow increased with the direction of flow. The effect of DRNA was more obvious in downflow than upflow and was affected by the external soil medium conditions and the abundance of microbial flora, reaching a maximum in the clay fine particle area at − 40 cm.

Conceptual model of nitrogen conversion in the interzone under different hydrodynamic conditions

By summarizing the content described in the above section, a conceptual model of the relevant processes of nitrogen conversion under the action of different water flow patterns can be constructed (Fig. 9).

The NH_4^+-N concentration in the simulated water samples that simulate the migration and transformation of nitrogen compounds during the infiltration of river water to replenish groundwater was relatively low, while the NO_3^--N

concentration was relatively high. The simulation fluid entered the oxidation layer to produce weak nitrification controlled by *Flavobacterium*, which converts NH_4^+-N to NO_3^--N. Nitrogen fixation controlled by *Azospira* also occurred in the oxidation layer. After entering the redox layer, DRNA and organic nitrogen mineralization mainly occurred. The role of DRNA in downflow was greater than that of organic nitrogen mineralization, which contributes more NH_4^+-N to nitrogen retention by the soil medium. Nitrification in this layer was minor, far weaker than DRNA. The effect of DRNA in this layer was controlled by *Desulfovibrio*, and some aerobic bacteria in *Pseudomonas* and *Bacillus* can also perform DRNA. Although there were denitrifying bacterial groups (*Sphingomonas*, *Pseudomonas*, and *Bacillus*) in downflow, the high-DO environment of the downflow simulation fluid affected denitrification, making downflow denitrification not as strong as that under upflow. The effects of denitrification and DRNA gradually reduced the concentrations of NO_3^--N and NO_2^--N in the water environment, and the adsorption and interception of NH_4^+-N by soil colloids significantly increased the content of NH_4^+-N in the soil medium. The abundance of bacterial groups in the weak reduction layer was significantly lower than that of the oxidizing layer and redox layer at the water-soil interface. According to the hydrodynamic conditions, the water flow velocity in the silt oxidation layer and clay redox layer reached 0.10 m/d and 0.01 m/d, respectively. The flow rate was lower than 0.40 m/d in the weak reduction layer of coarse sand. There was a longer HRT in the oxidation layer and the redox layer. The reaction time of the redox layer was 8.40 d, which was 30 times that of the weak reduction layer. The water flow conditions of the oxidation layer at the water-soil interface carried rich carbon sources, the clay redox layer had a rich organic matter content and high microbial diversity and abundance, and the reaction was fully carried out. The microbial abundance in the weak reduction layer was low, the HRT was short, and the reaction progress was weak. After a series of microbiologically controlled inorganic nitrogen conversion reactions, after 32 days of hydrodynamic action, the inorganic concentration of the effluent remained basically unchanged, and the NO_3^--N removal rate of the experimental effluent was as high as 99.3%.

The simulated groundwater recharge process is shown in the figure. Only NO_3^--N was carried in the simulated liquid, which first passed through the reduction layer, and denitrifying microbial communities related to nitrogen transformation, such as *Sphingomonas*, *Bacillus*, *Pseudomonas*, and *Aerobacter*, existed in this layer. In the low-oxygen environment (DO < 2 mg/L), strong denitrification occurred, and the concentration of NO_3^--N in the water gradually decreased. The concentration of NO_2^--N increased slightly and then decreased, which may be initially due to the rate-limiting process of NO_2^--N catalysis by nitrate reductase, after which the synthesis and catalytic action of nitrite reductase led to the transformation of NO_2^--N and a reduction in NO_2^--N concentration. In the reduction layer, *Azospira* also fixed N_2 in the air as it entered with water flow, converting it into organic nitrogen. In the redox layer, in addition to denitrification, organic nitrogen mineralization and DRNA occurred, which are controlled by some species of *Pseudomonas* and *Bacillus*. The clay area in the redox layer had a high organic matter content, and the HRT of water flowing through this area was longer, which made the microbial reaction more intense. The denitrifying bacteria at the bottom showed a stronger denitrification capacity under the influence of low-DO and reduction conditions. As flow entered the oxidation–reduction layer, denitrification was gradually weakened, while organic nitrogen mineralization and anammox were gradually enhanced. Then, along the direction of water flow, the NH_4^+-N in the process of Fe(III)-coupled anammox was oxidized in the weak oxidation layer, in which *Geobacter*-controlled iron respiration occurred, mainly generating N_2 and storing energy. In the weak oxidation layer, the abundance of bacteria was low, and the concentration of inorganic nitrogen was low. The low reaction rate kept the concentration of inorganic nitrogen basically stable in the water environment. After a series of inorganic conversion reactions controlled by microorganisms, the inorganic nitrogen concentration of the effluent remained basically unchanged after the end of the 32-day experiment, and the NO_3^--N removal rate of the experimental effluent was as high as 99.1%.

Conclusion

When the concentration of NO_3^--N in the experimental effluent was stable, the NO_3^--N removal rates were 99.1% and 99.3% under upflow and downflow modes, respectively. The denitrification under downflow (DO > 4.5 mg/L) was weaker than that under upflow (DO = 2.75 ± 0.75 mg/L) with the same carbon source. The DRNA effect of upflow was significantly lower than that of downflow.

Different G-S action modes resulted in different characteristics of nitrogen interception in soil colloidal media, and the interception of nitrogen in downwelling was greater than that in upwelling. The filling medium in the soil column included an area with fine clay particles; this area exhibited a prolonged HRT and had a more obvious effect on nitrogen accumulation in the soil medium.

Under upwelling, the main reactions in the − 50 ~ − 70-cm reduction layer were denitrification controlled by *Sphingomonas*, *Bacillus*, and *Aerobacter* and nitrogen fixation controlled by *Azospira*. In the redox layer of − 20 ~ − 50 cm, denitrification, organic nitrogen mineralization, anammox, strong soil colloid adsorption, and interception of nitrogen mainly occurred. Organic nitrogen mineralization was mainly controlled by some bacteria of

Pseudomonas and *Bacillus*. *Geobacter*-involved Fe(III)-coupled anammox occurred from 0 to − 20 cm.

In the 0 ~ − 20-cm oxidation layer under downwelling, nitrification was mainly controlled by *Flavobacterium*, and nitrogen fixation was mainly controlled by *Azospira*. DRNA action was dominated by some aerobic bacteria of *Pseudomonas* and *Bacillus*; denitrification controlled by *Pseudomonas*, *Sphingomonas*, and *Bacillus* occurred in the redox layer of − 20 ~ − 40 cm, and strong adsorption and retention of nitrogen by soil colloids occurred.

The upwelling and downwelling soil interfaces provided abundant carbon sources, which were conducive to the growth and development of microorganisms, and the abundance of microorganisms was high. The HRT in the fine clay area reached 8.40 d, and rich organic matter was provided, which promoted the extent of the microbial inorganic nitrogen transformation process.

Author contribution Lei Duan: Methodology, writing—original draft and editing, funding acquisition, supervision. Jinghui Fan: Formal analysis, data curation, writing—original draft. Yike Wang: Software, resources. Yakun Wu: Formal analysis, visualization. Chenchen Xie and Fei Ye: Methodology. Jiajia Lv and Mao Ming: Investigation. Yaqiao Sun: Writing—original draft and editing, supervision.

Funding This work was supported by the National Natural Science Foundation of China (No. 41877190, 41102150) and the Key Research and Development Program of Shaanxi (No. 2020ZDLSF06-04, 2021ZDLSF05-05).

Data availability Not applicable. In order to protect the privacy of my research data and that of the researchers involved, the original data will not be provided. The data are presented in various figures and tables in the manuscript.

Declarations

Ethical approval There are no ethical issues involved in the thesis.

Consent to participate My writers and I agreed to participate.

Consent to publish My writers and I agreed to publish.

Competing interests We declare that we have no financial and personal relationships with other people or organizations that can inappropriately influence our work; there is no professional or other personal interest of any nature or kind in any product, service, and/or company that could be construed as influencing the position presented in, or the review of, the manuscript entitled "Interaction mechanism between nitrogen conversion and the microbial community in the hydrodynamic heterogeneous interaction zone."

References

Agarwal M, Singh M, Hussain J (2019) Assessment of groundwater quality with special emphasis on nitrate contamination in parts of Gautam Budh Nagar district, Uttar Pradesh, India [J]. Acta Geochim 38(5):703–717. https://doi.org/10.1007/s11631-018-00311-z

Barnes RT, Sawyer AH, Tight DM, Wallace CD, Hastings MG (2019) Hydrogeologic controls of surface water-groundwater nitrogen dynamics within a tidal freshwater zone [J]. J Geophys Res Biogeosci 124(11):3343–3345. https://doi.org/10.1029/2019JG005164

Beggs RA, Hills DJ, Tchobanoglous G, Hopmans JW (2011) Fate of nitrogen for subsurface drip dispersal of effluent from small wastewater systems [J]. J Contam Hydrol 126(1–2):19–28. https://doi.org/10.1016/j.jconhyd.2011.05.007

Cao YR, Li MJ, Mao SJ, Li YQ, Zhu ZC, Tong L, Liu H (2021) Groundwater hydrochemistry and nitrogen distribution in the river-groundwater interaction zone of the lower Hanjiang River [J]. Earth Environ 49(05):463–471. https://doi.org/10.13869/j.cnki.rswc.2021.02.011

Chaudhary K, Cardenas MB, Deng W, Bennett BC (2011) The role of eddies inside pores in the transition from Darcy to Forchheimer flows [J]. Geophys Res Lett 38(38) https://doi.org/10.1029/2011GL050214

Chen QY, Zhao BJ, Yuan J, Zhang J, Tan X, Zhang QF (2018) Effects of artificial shading and nutrient addition on denitrifying activity and community structure of denitrifying bacteria in rivers [J]. Acta Ecol Sin 38(15):5566–5576 (CNKI:SUN:STXB.0.2018-15-030)

Chen XH (2007) Hydrologic connections of a stream-aquifer-vegetation zone in south-central Platte River valley, Nebraska [J]. J Hydrol 333(2–4):554–568. https://doi.org/10.1016/j.jhydrol.2006.09.020

Duan L (2010) Nitrogen pollution mechanism and safety assessment of groundwater quality in Guanzhong Basin [D]. Chang'anuniversity (In Chinese)

Duff JH, Triska FJ (2000) Nitrogen biogeochemistry and surface-subsurface exchange in streams [M]. https://doi.org/10.1016/B978-012389845-6/50009-0

Fang L, Tao W, Shi ZJ, Liu Y, Liu CF (2014) Study on bacterial diversity of coastal wetland sediments by metagenomics method [C]//. Abstract Collection of Papers of "Marine and Limnology Ecological Security under Global Change" Academic Exchange, p 153

Ge SJ, Peng YZ, Wang SY, Lu CC, Zhu YP (2012) Nitrite accumulation under constant temperature in anoxic denitrification process: the effects of carbon sources and COD/NO_3^-N [J]. Biores Technol 114:137–143. https://doi.org/10.1016/j.biortech.2012.03.016

Hou L, Min L, Carini SA, Gardner WS (2012) Transformation and fate of nitrate near the sediment-water interface of Copano Bay [J]. Cont Shelf Res 35:86–94. https://doi.org/10.1016/j.csr.2012.01.004

Huang B, Deng JB, Mu QL (2019) Bacterial communities in sediments of the western Yellow Sea and their responses to environmental factors [J]. J Ecol Environ 28(07):1423–1433. https://doi.org/10.16258/j.cnki.1674-5906.2019.07.016 (In Chinese)

Kraft B, Strous M, Tegetmeyer HE (2011) Microbial nitrate respiration-genes, enzymes and environmental distribution [J]. J Biotechnol 155(1):104–117. https://doi.org/10.1016/j.jbiotec.2010.12.025

Li JR, Wang L, Chen T, Liu CJ (2012) Experimental study on the effect of dissolved oxygen on nitrogen release in river sediment [J]. China's Rural Water Hydropower (05):32–34+38 (In Chinese)

Liu S, Hu BL, He ZF, Zhang B, Tian GM, Zheng P, Fang F (2015) Ammonia-oxidizing archaea have better adaptability in oxygenated/hypoxic alternant conditions compared to ammonia-oxidizing bacteria [J]. Appl Microbiol Biotechnol 99(20):8587–8596. https://doi.org/10.1007/s00253-015-6750-7

Liu YY, Li CX, Nelson WC, Shi L, Xu F, Liu YD, Yan AL, Zhong LR, Thompson C, Fredrickson JK, Zachara JM (2017) Effect of water chemistry and hydrodynamics on nitrogen transformation activity and microbial community functional potential in hyporheic zone sediment columns [J]. Environ Sci Technol 51:4877–4886. https://doi.org/10.1021/acs.est.6b05018

Li YL, Sun W, Yang ZR (2017) Sources, migration and transformation of nitrate in rivers in the middle reaches of Taizi River Basin [J]. Environ Sci 38(12):5039–5046. https://doi.org/10.13227/j.hjkx.201704238

Ma J, Song XR, Li L (2014) Effect of carbon source on NO_2^- accumulation and effluent pH value in denitrification process [J]. Chinese Environ Sci 34(10):2556–2561 (CNKI:SUN:ZGHJ.0.2014-10-019)

Marzadri A, Tonina D, Mckean JA, Tiedemann MB, Benjanker RM (2014) Multi-scale streambed topographic and discharge effects on hyporheic exchange at the stream network scale in confined streams [J]. J Hydrol 519:1997–2011. https://doi.org/10.1016/j.jhydrol.2014.09.076

Mermillod-Blondin F, Mauclaire L, Montuelle B (2005) Use of slow filtration columns to assess oxygen respiration, consumption of dissolved organic carbon, nitrogen transformations, and microbial parameters in hyporheic sediments [J]. Water Res 39(9):1687–1698. https://doi.org/10.1016/j.watres.2005.02.003

Peng CR, Chen L, Bi YH, Xia CX, Lei YM, Yang Y, Jian TZ, Hu ZY (2014) Effects of flood regulation of three Gorges Reservoir on algae community structure in Xiangxi River [J]. Chinese Environ Sci 34(07):1863–1871 (CNKI: SUN:ZGHJ.0.2014-07-043)

Rassam DW, Fellows CS, Hayr RD, Hunter H, Bloesch P (2006) The hydrology of riparian buffer zones; two case studies in an ephemeral and a perennial stream [J]. J Hydrol 325(1–4):308–324. https://doi.org/10.1016/j.jhydrol.2005.10.023

Repert DA, Underwood JC, Smith RL, Song BK (2015) Nitrogen cycling processes and microbial community composition in bed sediments in the Yukon River at Pilot Station [J]. J Geophys Res Biogeosci 119(12):2328–2344. https://doi.org/10.1002/2014JG002707

Robert SS, Thad SJ, Bartsch LA, Parr TB (2014) Particulate organic matter quality influences nitrate retention and denitrification in stream sediments: evidence from a carbon burial experiment [J]. Biogeochemistry 119(1–3):387–402. https://doi.org/10.1007/s10533-014-9975-0

Sawyer AH, Cardenas MB (2009) Hyporheic flow and residence time distributions in heterogeneous cross-bedded sediment [J]. Water Resour Res 45(8). https://doi.org/10.1029/2008WR007632

Shao L, Xu ZX, Jin W, Yin HL (2008) Rice husk as carbon source and biofilm carrier for water denitrification [J]. J Biotechnol 136(4):647–677. https://doi.org/10.1016/j.jbiotec.2008.07.1534

Shuai P, Cardenas MB, Knappett PSK, Bennett PC, Neilson BT (2017) Denitrification in the banks of fluctuating rivers: the effects of river stage amplitude, sediment hydraulic conductivity and dispersivity, and ambient groundwater flow [J]. Water Resour Res 53(9):7951–7967. https://doi.org/10.1002/2017WR020610

Song GD (2013) Key processes of nitrogen cycling in sediments from the East China Sea [D]. Doctoral dissertation, Ocean University of China, Qingdao (In Chinese)

Song J, Chen XH, Cheng C, Wang DM, Lackey SS, Xu ZX (2009) Feasibility of grain-size analysis methods for determination of vertical hydraulic conductivity of streambeds [J]. J Hydrol 375(3–4):428–437. https://doi.org/10.1016/j.jhydrol.2009.06.043

Song YJ, Ma L, Li M, Fu Y, Liang XY, Zhang HY, Wang XY, Guo HE (2020) Spatial distribution of nitrogen-fixing microorganisms in the rhizosphere of Phragmites australis in the Yellow River Delta [J]. J Henan Agric Univ 54(06):1026–1032+1040. https://doi.org/10.16445/j.cnki.1000-2340.20201130.001

Stonedahl SH, Sawyer AH, Stonedahl F, Reiter C, Gibson C (2018) Effect of heterogeneous sediment distributions on hyporheic flow in physical and numerical models [J]. Ground Water 56(6):935–946. https://doi.org/10.1111/gwat.12632

Su JJ, Liu BY, Liu CY (2001) Comparison of aerobic denitrification under high oxygen atmosphere by *Thiosphaera pantotropha* ATCC 35512 and *Pseudomonas stutzeri* SU2 newly isolated from the activated sludge of a piggery wastewater treatment system [J]. J Appl Microbiol 90(3):457–462. https://doi.org/10.1046/j.1365-2672.2001.01265.x

Su XS, Shi YK, Dong WH, Yang GQ, Wang H (2019) Advances in biogeochemical characteristics of hyporhedral zone [J]. J Earth Sci Environ 41(03):337–351. https://doi.org/10.3969/j.issn.1672-6561.2019.03.008

Tang Z, Zhang Y, Zeng L, Yuan Q, Na L (2019) Investigation and analysis of three nitrogen pollution in groundwater in Ledong, Hainan Province [J]. Agric Biotechnol 8(03):135–137+144. https://doi.org/10.19759/j.cnki.2164-4993.2019.03.032

Tao YL, Wen DH (2016) The process of bacterial nitrate dissimilation to ammonium and its potential position and influence in estuarine ecosystem [J]. Microbiol Bullet 43(001):172–181. https://doi.org/10.13344/j.microbiol.china.150288 (In Chinese)

Tatariw C, Chapman EL, Sponseller RA, Mortazavi B, Edmonds JW (2013) Denitrification in a large river: consideration of geomorphic controls on microbial activity and community structure [J]. Ecology 94(10):2249–2262. https://doi.org/10.1890/12-1765.1

Tonina D, De Barros FPJ, Marzadri A, Bellin A (2016) Does streambed heterogeneity matter for hyporheic residence time distribution in sand-bedded streams [J]. Adv Water Resour 96:120–126. https://doi.org/10.1016/j.advwatres.2016.07.009

Valiente N, Carrey R, Otero N, Soler A, Sanz D, Muñoz-Martín A, Jirsa F, Wanek W, Gómez-Alday JJ (2018) A multi-isotopic approach to investigate the influence of land use on nitrate removal in a highly saline lake-aquifer system [J]. Sci Total Environ 631–632:649–659. https://doi.org/10.1016/j.scitotenv.2018.03.059

Vince PK, Eugenio M-N, Hans EA, John PB, Martina JM, Perry GB (2018) A conceptual model for the analysis of multi-stressors in linked groundwater-surface water systems [J]. Sci Total Environ 627:880–895. https://doi.org/10.1016/j.scitotenv.2018.01.259

Wang LL, Li YL, Chen NX, Yu XQ, Xiao HS (2019) Experimental study on permeability characteristics of typical media in the Yellow River alluvial plain [J]. Geotech Invest Surv 47(08):36–42 (CNKI:SUN:GCKC.0.2019-08-006)

Wang Y, Li K, Tanaka T, Yang D, Inamura T (2016) Soil nitrate accumulation and leaching to groundwater during the entire vegetable phase following conversion from paddy rice [J]. Nutr Cycl Agroecosyst 106(3):325–334. https://doi.org/10.1007/s10705-016-9807-9

Wu C, Zou X, Wang H, He MY, Luo J, Ouyang GJ (2019) Study on soil water transport and nitrogen distribution under negative pressure irrigation [J]. J Irrig Drain 38(06):44–49 (CNKI:SUN:ZNSD.0.2012-05-010)

Wu ML, Nie MQ, Wang XC, Su JM (2008) Effect of Mn~(2+) on pyrene degradation by Flavobacterium FCN2 strain [J]. Environ Sci 29(7):1982–1985. https://doi.org/10.13227/j.hjkx.2008.07.041

Xu W, Hu P, Li YH, Li XM, Zhou SJ (2008) Advances in the mechanism of microbial iron respiration [J]. Chinese J Ecol 06:1037–1042 (CNKI:SUN:STXZ.0.2008-06-027)

Yabusaki SB, Wilkins MJ, Fang YL, Williams KH, Arora B, Bargar JR, Beller HR, Bouskill NJ, Brodie EL, Christensen JN, Conrad ME, Danczak RE, King E, Spycher NF, Steefel CI, Tokunaga TK, Versteeg RJ, Waichler SR, Wainwright HM (2017) Water table dynamics and biogeochemical cycling in a shallow, variably-saturated floodplain [J]. Environ Sci Technol 51(6):3307–3317. https://pubs.acs.org/10.1021/acs.est.6b04873

Yan YN, Ma T, Zhang JW, Liao M, Wang ZZ (2017) Transport and transformation of nitrate nitrogen under the interaction between groundwater and surface water [J]. Earth Sci 5:783–792 (CNKI:SUN:ZGHJ.0.2014-10-019)

Yu ZM, Wu GZ, Huang MX, Li LX (2021) Experimental study on nitrate nitrogen migration in fluvial soil under surface water-groundwater interaction [J]. Soil Water Conserv Res 28(2):67–73. https://doi.org/10.13869/j.cnki.rswc.2021.02.011

Zhang D, Cui RY, Fu B, Yang YX, Wang PL, Mao YT, Chen AQ, Lei BK (2019) Shallow groundwater table fluctuations affect bacterial communities and nitrogen functional genes along the soil profile in a vegetable field [J]. Appl Soil Ecol 146:1–8. https://doi.org/10.1016/j.apsoil.2019.103368

Zhang L, Wang SR, Wu ZH (2014) Coupling effect of pH and dissolved oxygen in water column on nitrogen release at water-sediment interface of Erhai Lake, China [J]. Estuar Coast Shelf Sci 149:178–186. https://doi.org/10.1016/j.ecss.2014.08.009 (In Chinese)

Zhang Q (2019) Effect of heterogeneity of hyporheic zone on nitrogen migration and transformation process under fluctuation of river level [D]. Harbin Institute of Technology. https://kns.cnki.net/KCMS/detail/detail.aspx?dbname=CMFD202001&filename=1019690453.nh

Zhang XJ, Zhao YL, Jin YD, Feng FY (2011) Bacterial diversity and phylogenetic analysis in sediments from Xiaokou Lake area of Wuliangsuhai Lake [J]. J Inner Mongolia Agric Univ (Natural Science Edition) 32(04):206–212 (CNKI:SUN:NMGM.0.2011-04-042)

Zhao L, Liu H (2018) Functional flora analysis of soil nitrogen cycling in fluctuating zone of Jianghan Oilfield [J]. Environ Sci Technol 41(11):49–53. https://doi.org/10.19672/j.cnki.1003-6504.2018.11.008 (In Chinese)

Zhao YJ, Deng YR, Lu HJ, Lv MC, Cheng Z (2021) Migration and transformation of three nitrogen in groundwater and antipollution effect of aquitard in North China Plain typical area [J]. Earth Environ Sci 760(1):012–038. https://doi.org/10.1088/1755-1315/760/1/012038

Zhong TY, Feng Q, Yu YY, Yang W, Sun YQ (2017) Effects of hydrodynamic effects on biofilm formation characteristics and quorum sensing system [J]. Water Purif Technol 36(11):26–32. https://doi.org/10.15890/j.cnki.jsjs.2017.11.005

Zhong XJ, Wang YJ, Tang JH, Zhang L, Zhou SG (2018) Ferric ammoxidation: a novel anaerobic ammoxidation process and its ecological significance [J]. J Fujian Agric For Univ (Natural Science Edition) 47(1):1–7. https://doi.org/10.13323/j.cnki.j.fafu(nat.sci.).2018.01.001

Zhuang W, Yang XQ, Yu XL, Yan QY, Lian YL, Wang C, Zhong QP, He ZL (2019) Progress in microbial-driven N_2O production and its mechanism in coastal wetlands [J]. Microbiol Bull 46(12):3440–3452. https://doi.org/10.13344/j.microbiol.china.190130